

This is a repository copy of *Hydrocarbon Removal in Power Plant Plumes Shows Nitrogen Oxide Dependence of Hydroxyl Radicals*.

White Rose Research Online URL for this paper:

<https://eprints.whiterose.ac.uk/147638/>

Version: Accepted Version

Article:

de Gouw, J. A., Parrish, D. D., Brown, S. S. et al. (15 more authors) (2019) Hydrocarbon Removal in Power Plant Plumes Shows Nitrogen Oxide Dependence of Hydroxyl Radicals. *Geophysical Research Letters*. pp. 7752-7760. ISSN 0094-8276

<https://doi.org/10.1029/2019GL083044>

Reuse

Items deposited in White Rose Research Online are protected by copyright, with all rights reserved unless indicated otherwise. They may be downloaded and/or printed for private study, or other acts as permitted by national copyright laws. The publisher or other rights holders may allow further reproduction and re-use of the full text version. This is indicated by the licence information on the White Rose Research Online record for the item.

Takedown

If you consider content in White Rose Research Online to be in breach of UK law, please notify us by emailing eprints@whiterose.ac.uk including the URL of the record and the reason for the withdrawal request.

de Gouw Joost A (Orcid ID: 0000-0002-0385-1826)
Parrish David D. (Orcid ID: 0000-0001-6312-2724)
Brown Steven S. S (Orcid ID: 0000-0001-7477-9078)
Edwards Peter M. (Orcid ID: 0000-0002-1076-6793)
Gilman Jessica B. (Orcid ID: 0000-0002-7899-9948)
Graus Martin (Orcid ID: 0000-0002-2025-9242)
Hanisco Thomas F. (Orcid ID: 0000-0001-9434-8507)
Keutsch Frank (Orcid ID: 0000-0002-1442-6200)
Kim Si-Wan (Orcid ID: 0000-0002-7889-189X)
Neuman J. Andrew (Orcid ID: 0000-0002-3986-1727)
Nowak John B. (Orcid ID: 0000-0002-5697-9807)
Pollack Ilana B. (Orcid ID: 0000-0001-7151-9756)
Roberts James M. (Orcid ID: 0000-0002-8485-8172)
Ryerson Thomas B. (Orcid ID: 0000-0003-2800-7581)
Veres Patrick R (Orcid ID: 0000-0001-7539-353X)
Warneke Carsten (Orcid ID: 0000-0003-3811-8496)
Wolfe Glenn (Orcid ID: 0000-0001-6586-4043)

Hydrocarbon Removal in Power Plant Plumes Shows Nitrogen Oxide Dependence of Hydroxyl Radicals

**J. A. de Gouw^{1,2}, D. D. Parrish^{1,3}, S. S. Brown^{2,3}, P. Edwards^{1,3,*}, J. B. Gilman³,
M. Graus^{1,3,†}, T. F. Hanisco⁴, J. Kaiser^{5,‡}, F. N. Keutsch⁵, S.-W. Kim^{1,3,#}, B. M.
Lerner^{1,3,§},
J. A. Neuman^{1,3}, J. B. Nowak^{1,3,i}, I. B. Pollack^{1,3,*}, J. M. Roberts³, T. B. Ryerson³,
P. R. Veres³, C. Warneke^{1,3}, G. M. Wolfe^{4,6}**

¹ Cooperative Institute for Research in Environmental Sciences, University of Colorado,
Boulder, CO

² Department of Chemistry and Biochemistry, University of Colorado, Boulder, CO

³ NOAA Earth System Research Laboratory, Boulder, CO

⁴ NASA Goddard Space Flight Center, Greenbelt, MD

⁵ Harvard University, Cambridge, MA

⁶ Joint Center for Earth Systems Technology, University of Maryland Baltimore County,
Baltimore, MD

Corresponding author: Joost de Gouw (Joost.deGouw@colorado.edu)

This article has been accepted for publication and undergone full peer review but has not been through the copyediting, typesetting, pagination and proofreading process which may lead to differences between this version and the Version of Record. Please cite this article as doi: 10.1029/2019GL083044

* Now with: University of York, United Kingdom

† Now with: University of Innsbruck, Innsbruck, Austria

‡ Now with: Georgia Institute of Technology, Atlanta, GA

Now with: Yonsei University, Seoul, South Korea

§ Now with: Aerodyne Research, Billerica, MA

¶ Now with: NASA Langley Research Center, Hampton, VA

• Now with: Colorado State University, Fort Collins, CO

Abstract

During an airborne study in the Southeast U.S., measured mixing ratios of biogenic hydrocarbons were systematically lower in air masses containing enhanced nitrogen oxides from power plants, which we attribute to increased concentrations of hydroxyl (OH) radicals within the power plant plumes. Plume transects at successively further downwind distances provide a decreasing gradient of nitrogen oxides (NO_x) concentrations, which together with the implied loss rates of isoprene, constrains the OH dependence on NO_x . We find that OH concentrations were highest at nitrogen dioxide concentrations near 1-2 ppbv and decreased at higher and at lower concentrations. These findings agree with the dependence of OH on NO_x concentrations expected from known chemical reactions but are not consistent with some studies reporting direct OH measurements higher than expected in regions of the atmosphere with low NO_x ($\text{NO} < 0.08$ ppbv and $\text{NO}_2 < 0.46$ ppbv) and high biogenic hydrocarbon emissions.

Plain Language Summary

Hydroxyl radicals (OH) are the main chemical species that removes trace gases from the atmosphere. They determine the atmospheric lifetime of some greenhouse gases and chemicals involved with the destruction of the stratospheric ozone layer. Hydroxyl reactions also play an important role in air pollution chemistry. Measuring hydroxyl radicals is very challenging because of their high reactivity and low concentrations. Some recent measurements have shown unexpectedly high concentrations in relatively clean conditions. In this work, we indirectly estimated the dependence of hydroxyl radicals on the concentration of nitrogen oxides downwind from power plants in the Southeast U.S. We observed that mixing ratios of isoprene, a reactive hydrocarbon released from deciduous trees to the atmosphere, were systematically lower in power plant plumes, caused by higher hydroxyl radical concentrations at the elevated nitrogen oxide concentrations. These findings can be explained by known chemical reactions but are not consistent with some studies that found unexpectedly high hydroxyl concentrations in relatively clean conditions.

Key Points:

- Isoprene was found to be reduced in power-plant plumes in the Southeast U.S. because of enhanced removal by hydroxyl (OH) radicals.
- Observations at different downwind distances from two power plants allow the nitrogen-oxide (NO_x) dependence of OH to be constrained.
- The NO_x dependence of OH is explained by known photochemistry, in contrast with some studies based on direct measurements of OH.

1 Introduction

Reaction with hydroxyl radicals (OH) is the primary removal mechanism for most atmospheric trace gases. Hydroxyl radicals control the atmospheric lifetimes of long-lived trace gases such as the greenhouse gas methane and several of the halogenated compounds that affect stratospheric ozone. Secondary pollutants including ozone (O₃) and aerosol can be formed from OH oxidation of volatile organic compounds (VOCs) in the presence of nitrogen oxides (NO+NO₂ = NO_x), thereby affecting regional air quality. OH concentrations depend on photolysis rates, concentrations of NO_x, VOCs, carbon monoxide (CO) and OH precursors such as ozone, formaldehyde (HCHO) and others. The known photochemical reactions predict lower OH at both low and high NO_x with OH at a maximum at an intermediate NO_x concentration (Ehhalt & Rohrer, 2000; Kuhn et al., 2007; McKeen et al., 1997; Spivakovsky et al., 2000).

Over the last decade, several direct OH measurements have shown unexpectedly high concentrations. For example, a study in the Amazon showed relatively high OH concentrations in air masses with low levels of NO_x and significant concentrations of isoprene, a highly reactive hydrocarbon released by vegetation (Lelieveld et al., 2008). A study in the Pearl River Delta, China found 3-5 times higher OH concentrations than modeled, and concluded that high concentrations of an unknown species must be present to regenerate OH from peroxy radicals (HO₂ and RO₂, where R represents an organic group) without the conversion of NO into NO₂ (Hofzumahaus et al., 2009). These and other observations were synthesized in a paper that concluded that OH concentrations do not decrease at low NO_x (NO<0.08 ppbv and NO₂<0.46 ppbv), but remain at a maximum as NO_x decreases (Rohrer et al., 2014). These conclusions have far-reaching implications as they affect estimates of the global lifetime of methane and the emission source strengths of isoprene and other biogenic hydrocarbons required to explain their observed concentrations. These conclusions also affect the predicted concentrations of products formed from biogenic hydrocarbon oxidation, e.g., formaldehyde and organic aerosol.

Theoretical chemistry modeling suggested that HO_x (OH+HO₂) recycling reactions involving low-NO_x products from isoprene oxidation could explain the higher than expected OH concentrations (Peeters et al., 2009). Laboratory measurements showed that such radical recycling reactions indeed exist, but also that the efficiency is not high enough to explain the high OH concentrations observed in the tropics (Crouse et al., 2011; Fuchs et al., 2013). Furthermore, some OH measurements suffer from interferences in regions of the atmosphere with high biogenic emissions (Feiner et al., 2016; Mao et al., 2012). At present, no consensus exists whether such interferences are common to other OH measurement instruments, and thereby could generally explain the high observed levels of OH in low-NO_x environments (Fittschen et al., 2019; Rohrer et al., 2014).

Indirect methods based on the removal of trace gases and the formation of products also constrain OH concentrations. For example, decreasing trends in methyl chloroform, which was mostly phased out by the Montreal Protocol, have been used to study trends in globally averaged OH (Montzka et al., 2011). Measurements of glyoxal provided a constraint on OH concentrations at a forested site (Huisman et al., 2011). Measurements of isoprene and its oxidation products in the Amazon under varying NO_x conditions showed that OH concentrations increase with NO_x up to mixing ratios of 3 ppbv (Liu et al., 2018).

In this work, we examine the dependence of OH concentrations on NO_x by contrasting airborne observations inside and outside of power plant plumes transported over a region in the Southeast U.S. with high and geographically uniform emissions of biogenic VOCs. Concentrations of OH were not directly measured, but gradients in the concentrations

of OH across power plant plumes are inferred from changes in the concentrations of the highly reactive biogenic VOCs isoprene and monoterpenes, whose primary sink is removal by OH. We show that isoprene and monoterpenes were systematically lower in power plant plumes, as a result of higher OH concentrations, and that their oxidation products (notably formaldehyde, whose dominant source is isoprene oxidation in forested regions) were systematically enhanced. Using these observations, we derive the dependence of OH concentrations on NO_x and compare to previous work.

2 Airborne Measurements During SENEX

Measurements were made from the NOAA WP-3D research aircraft during the NOAA Southeast Nexus (SENEX) project in June and July, 2013. The aircraft was operated out of the Smyrna/Rutherford County airport in Smyrna, Tennessee. Flight objectives included regional surveys across the Southeast U.S. to study the interactions of abundant biogenic VOCs with anthropogenic emissions (motor vehicles in urban areas, power plants, industrial sources) to form secondary pollutants such as ozone and aerosol. The aircraft was equipped with instruments to characterize the chemical composition of trace gases and aerosol, as well as the size distribution, radiative and cloud-nucleating properties of the aerosol (Warneke et al., 2016). The measurements used in this analysis are summarized in Table S1; additional measurements onboard the NOAA WP-3D that are not used in this analysis, are omitted from this table.

VOCs were measured using proton-transfer-reaction mass spectrometry (PTR-MS) (de Gouw & Warneke, 2007) and post-flight gas chromatographic analyses of whole air samples collected in flight (Lerner et al., 2017). The PTR-MS was operated in selected-ion mode, resulting in one data point for each VOC every ~15 seconds. The measurements of isoprene and monoterpenes are compared in Figure S1. On average, the two measurements agreed within 7% for isoprene and 9% for total monoterpenes. These biogenic hydrocarbons are highly variable in the daytime boundary layer due to a strong variability in emissions (land-use, cloudiness), turbulent mixing and chemistry. This variability is responsible for much of the scatter in Figure S1 between the measurements of isoprene and monoterpenes by different techniques that are not perfectly coincident in time. Methacrolein (MACR) and methyl vinyl ketone (MVK) are isoprene oxidation products with the same molecular mass that are measured as a sum by the PTR-MS instrument.

3 Results and Discussion

3.1 Steady-state analysis of biogenic VOC concentrations

Emissions from power plants were intercepted on multiple flights during SENEX in 2013 (Warneke et al., 2016). The measurements on 16 June 2013 provide an excellent case for studying the composition of power plant plumes as a function of the time since emission. Enhancements in NO_2 were observed over and downwind from Atlanta, and downwind from two of the largest point sources of NO_x in the area, i.e. the Scherer and Harllee Branch power plants to the southeast of Atlanta. The Scherer plant is the largest coal plant in the U.S. The Harllee Branch plant closed in 2015. The emissions from these two facilities were each sampled at ~450 m above ground within the PBL at five different distances from the source, and the chemical evolution of the plumes provides the basis for the analysis presented here (Figure 1). Data from an example plume intercept are also shown; enhancements in NO and NO_2 were observed between 12:52 and 12:54 PM Eastern Standard Time (EST). Within the plume there was a clear minimum in the observed isoprene mixing ratios; the average isoprene was 1.84 ± 0.10 ppbv before, 0.55 ± 0.08 ppbv inside and 1.64 ± 0.20 ppbv after the

plume intercept, where the indicated uncertainties give the 1- σ confidence limits of the means, calculated from the standard deviation divided by the square root of the number of data points. In the plume, formaldehyde concentrations were enhanced simultaneously with the depletion of isoprene. Depletion of isoprene in power plant plumes was observed on multiple other flights; two more examples are shown in Figures S2 and S3 in the Supplementary Information. As discussed in more detail below, we attribute the depletion of isoprene to enhanced OH concentrations at the higher NO_x concentrations in the plume, and the enhancement in formaldehyde to secondary formation from isoprene.

Average plume compositions are calculated by averaging the data over the central one-minute measurement time (~6 km horizontal distance) inside the plume. These compositions are then compared with the observations outside the plumes, calculated from two-minute windows before and after the plume. For the June 16 flight, the intervals used for computing the average composition before, inside and after plume intercepts are shown in Figure 1. The mixing ratios of isoprene are highly variable due to its short lifetime, heterogeneous surface emissions and vertical mixing, which are uncorrelated with the power plant emissions themselves. Consequently, the correlation between different trace gases (Ryerson et al., 2001) is limited and average plume composition was used instead.

The power plant plumes shown in Figure 1 traversed an area with dense, mixed forests typical of the Southeast U.S., which are known to be strong emitters of isoprene and other biogenic hydrocarbons (Warneke et al., 2010). Isoprene has a lifetime of ~0.5 hour in the sunlit atmosphere at an OH concentration of 5×10^6 molecules cm⁻³. This lifetime is shorter than the transport times of most of the power plant plumes sampled in this work (~4 hours for the plume transect shown in Figure 1). At steady state, isoprene concentrations [ISOP] are determined by the balance between isoprene emissions beneath the plume (ISOP_{em}) and loss of isoprene to reaction with OH within the plume. This balance defines a relationship between the depth of the mixing layer (BL_{height}), the concentration of OH and the rate coefficient for the reaction between isoprene and OH (k_{OH}) (Warneke et al., 2010):

$$[\text{ISOP}] = \frac{\text{ISOP}_{\text{em}}}{\text{BL}_{\text{height}} \times k_{\text{OH}} \times [\text{OH}]} \quad (1)$$

As isoprene emissions and boundary layer height do not vary systematically across the plumes, we attribute the depletion in isoprene to a higher concentration of OH in the plume. The enhanced formaldehyde is consistent with this explanation: formaldehyde is not directly emitted from power plants but is efficiently formed from the reaction between isoprene and OH (Wolfe et al., 2016). Monoterpenes react with OH at a rate similar to that of isoprene, so their concentrations can also be estimated from a steady-state analysis analogous to Equation (1). The validity of Equation (1) is investigated in more detail in section 3.3 below.

3.2 Chemical evolution of power plant plumes

Comparisons of average plume compositions with those outside the plume (see Figure 1 and the Methods Section for more details) can elucidate the chemical processes occurring within the plume, including the dependence of OH on NO_x concentrations. The results for NO₂, isoprene, formaldehyde and monoterpenes are shown in Figure 2, and the results for several other species formed in biogenic VOC oxidation (NO, nitric acid, methyl vinyl ketone (MVK) and methacrolein (MACR), peroxyacetyl nitrate and ozone) are shown in the Supplementary Material (Figure S4). The average NO₂ in the plume decreased rapidly with distance due to a combination of chemical reaction and dilution. The plume intercepts nearest to Harllee Branch and Scherer were 7.6 km and 22 km from the respective sources. Higher NO_x concentrations were observed during the first downwind intercept of the Harllee Branch

plume compared to the first intercept of the Scherer plume. The emissions of NO_x from these plants were measured by continuous emission monitoring systems (CEMS) at the stack level and are shown in Figure S5.

Three different chemical regimes explain the downwind trace gas concentrations observed in these power plant plumes:

1. Close to the emission source, NO_x is high enough to titrate a fraction of the ozone and limit the lifetime and concentration of OH via the $\text{OH}+\text{NO}_2$ termination reaction. As a result, isoprene is not significantly lower inside the plume, and enhancements in the isoprene oxidation products are not yet observed. There is no enhancement in formaldehyde, illustrating that there is no direct emission from a coal-fired power plant. Only the first Harlee Branch plume intercept fits this situation (NO was 9 ppbv, NO_2 was 11 ppbv). The first intercept of the Scherer plume was further downwind and is better described by the next chemical regime.
2. After NO_x has been diluted and oxidized during transport, it reaches a concentration at which hydroperoxy radicals are efficiently recycled back to OH radicals. In this regime, OH concentrations are higher, and as a result, isoprene is lower inside the plumes than outside. Additionally, inside the plume the products of isoprene oxidation such as formaldehyde are enhanced (Fig. 2), and ozone, peroxyacetyl nitrate (PAN) and nitric acid are formed (Fig. S4). This chemical regime best describes the 2nd and 3rd plume intercept of the Harlee Branch plume, and the 1st through 3rd intercept of the Scherer plume (NO ranged from 0.1-2.2 ppbv, NO_2 ranged from 0.6-5.6 ppbv); this last-mentioned intercept is the example shown in Figure 1.
3. After NO_x has been decreased even further, HO_x radicals are less efficiently recycled. Hydroxyl concentrations in the plume are no longer much enhanced over their concentrations outside the plume. As a result, isoprene concentrations inside the plume approach those outside. The products of isoprene oxidation are still enhanced due to their longer lifetimes compared to isoprene. This regime describes the observations in the 4th and 5th intercept of both the Harlee Branch and Scherer plumes ($\text{NO} < 0.055$ ppbv, $\text{NO}_2 < 0.30$ ppbv).

These three chemical regimes explain the depletion in isoprene observed within the plumes downwind from Harlee Branch and Scherer as well as the formation of the products formaldehyde (Figure 2), nitric acid, PAN and ozone (Figure S4). No clear enhancement was observed for MVK and MACR; these compounds react more efficiently with OH than formaldehyde, so their enhanced formation in the plumes is counteracted by their enhanced removal. Also, it was recently discovered that a low- NO_x oxidation product from isoprene is detected at the same mass as MVK and MACR (Rivera Rios et al., 2014), which may also obscure their enhancement in the plume.

Monoterpenes were also depleted downwind from Harlee Branch and Scherer, and the depletion exhibited a similar dependence on downwind distance as for isoprene (Figure 2). The monoterpene concentrations were much lower than isoprene and at these low concentrations, instrumental noise in the measurement contributes substantially to the variability in the observations (de Gouw & Warneke, 2007).

Based on the observations made downwind from the Scherer and Harlee Branch power plants, we can derive the NO_x dependence of OH in the plumes. Using Equation (1), and assuming that isoprene emissions and boundary layer height are the same inside and outside of the plume, we define:

$$\text{OH enhancement ratio} = \frac{[\text{OH}]_{\text{inside}}}{[\text{OH}]_{\text{outside}}} = \frac{[\text{ISOP}]_{\text{outside}}}{[\text{ISOP}]_{\text{inside}}} \quad (2)$$

The OH enhancement ratios according to Equation (2) are shown in Figure 3 as a function of average NO₂, using both isoprene and monoterpene measurements. Data are shown as a function of NO₂ for direct comparison with the literature (Rohrer et al., 2014). Both graphs show that the largest OH enhancement ratio occurs at intermediate NO₂ concentrations near 1-2 ppbv. At higher (closer to the power plant) and lower (further away from the power plant) NO₂ mixing ratios, OH is not as strongly enhanced. The OH+NO₂ reaction to form nitric acid limits OH concentrations at high NO₂, and low concentrations of NO limit the recycling of hydroperoxy radicals to OH at low NO₂ (McKeen et al., 1997). The peak enhancement ratio in OH is estimated to be 5.9±1.1 from the isoprene measurements and 3.9±1.5 from the monoterpene measurements, where the uncertainties are determined from lognormal fits to the data shown in Figure 3. These peak enhancement ratios agree within the uncertainties of the analyses. The monoterpene measurements by PTR-MS are much closer to the instrument detection limit than the isoprene measurements. If the 11-pptv offset inferred from the monoterpene data inter-comparison in Figure S1 were due to a different species than monoterpenes, then the peak OH enhancement inferred from the monoterpene measurements (Figure 3) would be higher (5.7±1.6) and would agree more closely with the isoprene result (5.9±1.1).

The dependence of OH on NO₂ concentrations inferred from the analysis in Figure 3 is consistent with several previous observations, including the Tropospheric OH Photochemistry Experiment (Eisele et al., 1997), measurements made during the Biosphere Effects on Aerosols and Photochemistry Experiment II (BEARPEX09) (Mao et al., 2012), measurements made at a ground site during the SENEX study (Feiner et al., 2016) and with the OH dependence on NO₂ predicted from well-known chemical reactions in the troposphere (McKeen et al., 1997). Indirect evidence for increased oxidation rates of VOCs at enhanced NO_x concentrations was obtained downwind from Manaus in the Amazon during GoAmazon2014/5 (Shrivastava et al., 2019). Our analysis does not provide evidence for higher than expected OH concentrations at lower NO_x concentrations as suggested by the recent summary of OH measurements (Rohrer et al., 2014). That study summarized data from a U.S. deciduous forest (Tan et al., 2001), the Amazon (Lelieveld et al., 2008), and a tropical forest in Borneo (Whalley et al., 2011). Between these studies the average daytime NO mixing ratios ranged from 0.013-0.08 ppbv and NO₂ ranged from 0.13-0.46 ppbv. Our observations furthest away from the power plants are in this same range (NO<0.055 ppbv and NO₂<0.30 ppbv). In Rohrer et al. [2014], the average dependence of OH on NO₂ followed a very similar trend as observed here at high NO_x but measured OH did not decrease with NO₂ at low NO_x. If the average NO₂ dependence of OH concentrations according to Rohrer et al. [2014] held for the present study, there would have been no gradients in isoprene in either the downwind or crosswind directions across the power plant plumes, except very close to the source, where OH would have been lower and isoprene higher inside the plume.

It should be noted that the summary of OH measurements by [Rohrer et al., 2014] was limited to those data sets with total OH reactivities of the combined hydrocarbons above 10 s⁻¹, which is not the case for all air masses described in this work. For the Scherer and Harlee Branch plumes observed 16 June 2013, the combined OH reactivity calculated from isoprene, monoterpenes, methyl vinyl ketone + methacrolein and formaldehyde varied between 4-7 s⁻¹ outside of the plumes and from 2-4 s⁻¹ inside the plumes due primarily to the depletion of isoprene. Nevertheless, a depletion of isoprene in power plant plumes was also observed in air masses that did have >10 s⁻¹ hydrocarbon reactivity. An example is shown in

Figure S3, in which case the OH reactivity was above 12 s^{-1} immediately preceding the plume intercept.

3.3 Possible complicating issues

The analysis presented here is based on indirect determinations of OH concentrations from relationships between observed concentrations of relatively easily measured species, and any influence from possible interferences in OH measurements is avoided. We discuss some complicating issues with the present analysis here, with more details included in the Supplementary Information.

Equation (1) describes the dependence of average isoprene concentration on average OH concentration when steady state is achieved. In the atmosphere, isoprene is turbulently mixed in the daytime boundary layer leading to a strong variability in time and location of both isoprene and OH (Kaser et al., 2015). This interplay between turbulent mixing and chemistry has been studied in a large eddy simulation (LES) model for conditions typical of the Southeast U.S. (Kim et al., 2012). As discussed in the Supplementary Material, the results from the LES model (i) provide justification for the use of Equation (1) that relates mean isoprene and OH concentrations, and (ii) explain the strong variability in isoprene observed in the daytime boundary layer over the eastern U.S.

The steady-state assumption underlying Equation (1) is justified at relatively high OH concentrations. At lower OH concentrations characteristic of chemical regimes 1 and 3 discussed above, the approach to steady state is slower. Thus, the shape of the OH enhancement ratio dependence shown in Figure 3 may be somewhat distorted due to departures from steady-state conditions at low and high NO_2 , with the OH maximum possibly shifted. However, these distortions cannot be large, as the low OH concentrations within the plume are not much different from those outside. Comprehensive plume dispersion modeling that includes detailed isoprene chemistry may give more definitive results but are beyond the scope of this data-focused analysis.

A coincidence between the plume trajectory and lower surface emissions or variations in vertical transport could possibly produce isoprene gradients not related to chemistry within the plume. The measured vertical wind speeds did not show systematic variations across the plume intercepts (Figure S6), which rules out enhanced or depressed turbulence. In addition, the surface emissions of isoprene did not have systematic gradients across the plume, which was verified by overlaying the plume intercept locations with emissions and satellite maps. Further, as mentioned before, depletion of isoprene in power plant plumes was observed on multiple flights. In addition, a reduction in isoprene concentrations was often observed downwind from urban areas; in those cases, however, a reduction in isoprene emissions underneath the plume cannot be easily ruled out (Kuhn et al., 2010).

Ozone and formaldehyde are secondary products of isoprene oxidation, which were formed in the Scherer and Harlee Branch plumes (Figure S4). These two species themselves accelerate chemical transformations in the plumes. However, as discussed in the Supplementary Information, the enhanced radical production that can be attributed to these species is small compared with the enhancement in OH that is attributed to the radical recycling by NO_x . Another radical precursor that was enhanced in the plumes was nitrous acid (HONO) (Neuman et al., 2016). HONO was most enhanced (by an average of ~ 70 pptv) during the first intercept of the Harlee Branch plume, which is not when the OH enhancement in the plume was highest. The enhanced radical production from HONO is further discussed in the Supplementary Information and was found to be small.

Finally, aerosol formation downwind from the Scherer and Harllee Branch power plants was studied and presented elsewhere (Xu et al., 2016). Emissions of SO₂ from Harllee Branch were much higher and, consequently, more sulfate aerosol as well as organic aerosol derived from isoprene were formed in that plume. Nevertheless, the present analysis suggests that the removal of isoprene oxidation products from the gas phase did not significantly alter the OH reactivity in the Harllee Branch plume relative to the Scherer plume, which is not unexpected given the dominant contributions of isoprene, monoterpenes, methyl vinyl ketone, methacrolein and formaldehyde to the total OH reactivity (Kaiser et al., 2016).

4 Conclusions

Airborne measurements in power plant plumes in the Southeast U.S. constrain the NO_x dependence of OH concentrations. We find that the OH dependence on NO₂ is consistent with well-known chemical reactions in the troposphere (McKeen et al., 1997). Our analysis does not provide evidence for higher than expected OH concentrations at lower NO_x concentrations as suggested by a recent summary of OH measurements (Rohrer et al., 2014). The apparent disagreement between the current findings and those obtained from some direct measurements of OH is important to resolve as it has major implications for global atmospheric chemistry and climate. Higher than expected OH concentrations in low-NO_x environments with high isoprene emissions such as the tropics would significantly affect the modeled lifetime of the greenhouse gas methane. High OH concentrations at low NO_x would also require that isoprene emissions are much larger than currently understood to explain the observed isoprene mixing ratios, which has far-reaching implications for the budget of isoprene and its oxidation products (formaldehyde, organic aerosol). Plume dispersion and large-eddy simulation models may provide further insights into the radical recycling processes observed in the laboratory (Crouse et al., 2011; Fuchs et al., 2013) and their relevance to the present observations. Finally, possible OH measurement issues require further investigation [Mao et al., 2012; Feiner et al., 2016; Fittschen et al., 2019].

Acknowledgments, and Data

The SENEX data used in this study are publicly available at <http://www.esrl.noaa.gov/csd/groups/csd7/measurements/2013senex/P3/DataDownload/>. We acknowledge helpful discussions with Michael Trainer, Hendrik Fuchs and Keding Lu. This work was supported by NOAA's Health of the Atmosphere and Atmospheric Chemistry and Climate Programs. We are thankful for the staff at the NOAA Aircraft Operations Center and the WP-3D flight crew for help in instrumenting the aircraft and for conducting the flights. The formaldehyde measurements were made possible with financial support from the STAR grant program of the U.S. EPA (3540601). This research has not been subjected to EPA review and therefore does not necessarily reflect the views of the agency, and no official endorsement should be inferred. J. Kaiser acknowledges support from NASA Headquarters under the NASA Earth and Space Science Fellowship Program – grant NNX14AK97H.

References

- Crouse, J. D., F. Paulot, H. G. Kjaergaard, and P. O. Wennberg (2011), Peroxy radical isomerization in the oxidation of isoprene, *Phys. Chem. Chem. Phys.*, *13*(30), 13607–13613, doi:10.1039/c1cp21330j.
- de Gouw, J. A., and C. Warneke (2007), Measurements of volatile organic compounds in the Earth's atmosphere using proton-transfer-reaction mass spectrometry, *Mass Spec. Rev.*, *26*(2), 223–257, doi:10.1002/mas.20119.
- Ehhalt, D. H., and F. Rohrer (2000), Dependence of the OH concentration on solar UV, *J. Geophys. Res.*, *105*, 3565–3571.
- Eisele, F. L., G. H. Mount, D. J. Tanner, A. Jefferson, R. Shetter, H. Harder, and E. J. Williams (1997), Understanding the production and interconversion of the hydroxyl radical during the Tropospheric OH Photochemistry Experiment, *J. Geophys. Res.*, *102*, 6457–6465.
- Feiner, P. A. et al. (2016), Testing Atmospheric Oxidation in an Alabama Forest, *J. Atmos. Sci.*, *73*(12), 4699–4710, doi:10.1175/JAS-D-16-0044.1.
- Fittschen, C., M. Al Ajami, S. Batut, V. Ferracci, S. Archer-Nicholls, A. T. Archibald, and C. Schoemaeker (2019), ROOOH: a missing piece of the puzzle for OH measurements in low-NO environments? *Atmos. Chem. Phys.*, *19*(1), 349–362, doi:10.5194/acp-19-349-2019.
- Fuchs, H. et al. (2013), Experimental evidence for efficient hydroxyl radical regeneration in isoprene oxidation, *Nature Geosci.*, *6*, 1023–1026, doi:10.1038/ngeo1964.
- Hofzumahaus, A. et al. (2009), Amplified Trace Gas Removal in the Troposphere, *Science*, *324*(5935), 1702–1704, doi:10.1126/science.1164566.
- Huisman, A. J. et al. (2011), Photochemical modeling of glyoxal at a rural site: observations and analysis from BEARPEX 2007, *Atmos. Chem. Phys.*, *11*, 8883–8897.
- Kaiser, J. W., Skog, K. M., Baumann, K., Bertman, S. B., Brown, S. S., Brune, W. H., et al. (2016). Speciation of OH reactivity above the canopy of an isoprene-dominated forest. *Atmos. Chem. Phys.*, *16*, 9349–9359, <https://doi.org/10.5194/acp-2015-1006>.
- Kaser, L. et al. (2015), Chemistry – turbulence interactions and mesoscale variability influence the cleansing efficiency of the atmosphere, *Geophys. Res. Lett.*, *42*, 10894–10903.
- Kim, S.-W., M. C. Barth, and M. Trainer (2012), Influence of fair-weather cumulus clouds on isoprene chemistry, *J. Geophys. Res.-Atmos.*, *117*(D10), D10302, doi:10.1029/2011JD017099.
- Kuhn, U. et al. (2007), Isoprene and monoterpene fluxes from Central Amazonian rainforest inferred from tower-based and airborne measurements, and implications on the atmospheric chemistry and the local carbon budget, *Atmos. Chem. Phys.*, *7*, 2855–2879.

- Kuhn, U. et al. (2010), Impact of Manaus City on the Amazon Green Ocean atmosphere: ozone production, precursor sensitivity and aerosol load, *Atmos. Chem. Phys.*, *10*(19), 9251–9282, doi:10.5194/acp-10-9251-2010.
- Lelieveld, J. et al. (2008), Atmospheric oxidation capacity sustained by a tropical forest, *Nature*, *452*(7188), 737–740, doi:10.1038/nature06870.
- Lerner, B. M. et al. (2017), An Improved, Automated Whole-Air Sampler and Gas Chromatography Mass Spectrometry Analysis System for Volatile Organic Compounds in the Atmosphere, *Atmos. Meas. Tech.*, *10*, 291–313, doi:10.5194/amt-10-291-2017.
- Liu, Y. et al. (2018), Isoprene photo-oxidation products quantify the effect of pollution on hydroxyl radicals over Amazonia, *Science Advances*, *4*(4), doi:10.1126/sciadv.aar2547.
- Mao, J. et al. (2012), Insights into hydroxyl measurements and atmospheric oxidation in a California forest, *Atmos. Chem. Phys.*, *12*(17), 8009–8020, doi:10.5194/acp-12-8009-2012.
- McKeen, S. A. et al. (1997), Photochemical modeling of hydroxyl and its relationship to other species during the Tropospheric OH Photochemistry Experiment, *J. Geophys. Res.*, *102*, 6467–6493.
- Montzka, S. A., M. Krol, E. J. Dlugokencky, B. Hall, P. Jockel, and J. Lelieveld (2011), Small Interannual Variability of Global Atmospheric Hydroxyl, *Science*, *331*(6013), 67–69.
- Neuman, J. A., Trainer, M., Brown, S. S., Min, K. E., Nowak, J. B., Parrish, D. D., et al. (2016). HONO emission and production determined from airborne measurements over the Southeast U.S. *J. Geophys. Res.-Atmos.*, *121*, 9237–9250, <https://doi.org/10.1002/2016JD025197>.
- Peeters, J., T. L. Nguyen, and L. Vereecken (2009), HOx radical regeneration in the oxidation of isoprene, *Phys. Chem. Chem. Phys.*, *11*, 5935–5939.
- Rivera Rios, J. C. et al. (2014), Conversion of hydroperoxides to carbonyls in field and laboratory instrumentation: Observational bias in diagnosing pristine versus anthropogenically controlled atmospheric chemistry, *Geophys. Res. Lett.*, *41*, 8645–8651, doi:10.1002/2014GL061919.
- Rohrer, F. et al. (2014), Maximum efficiency in the hydroxyl-radical-based self-cleansing of the troposphere, *Nature Geosci.*, *7*, 559–563, doi:10.1038/ngeo2199.
- Ryerson, T. B. et al. (2001), Observations of ozone formation in power plant plumes and implications for ozone control strategies, *Science*, *292*, 719–723.
- Shrivastava, M. et al. (2019), Urban pollution greatly enhances formation of natural aerosols over the Amazon rainforest, *Nature Communications*, 1–12, doi:10.1038/s41467-019-08909-4.
- Spivakovsky, C. M. et al. (2000), Three-dimensional climatological distribution of tropospheric OH: Update and evaluation, *J. Geophys. Res.-Atmos.*, *105*, 8931–8980.

Tan, D., Faloon, I., Simpas, J. B., Brune, W. H., Shepson, P. B., Couch, T. L., et al. (2001). HO_x budgets in a deciduous forest: Results from the PROPHET summer 1998 campaign. *J. Geophys. Res.-Atmos.*, *106*, 24407–24427, <https://doi.org/10.1029/2001JD900016>.

Warneke, C. et al. (2010), Biogenic emission measurement and inventories determination of biogenic emissions in the eastern United States and Texas and comparison with biogenic emission inventories, *J. Geophys. Res.-Atmos.*, *115*, D00F18, doi:10.1029/2009JD012445.

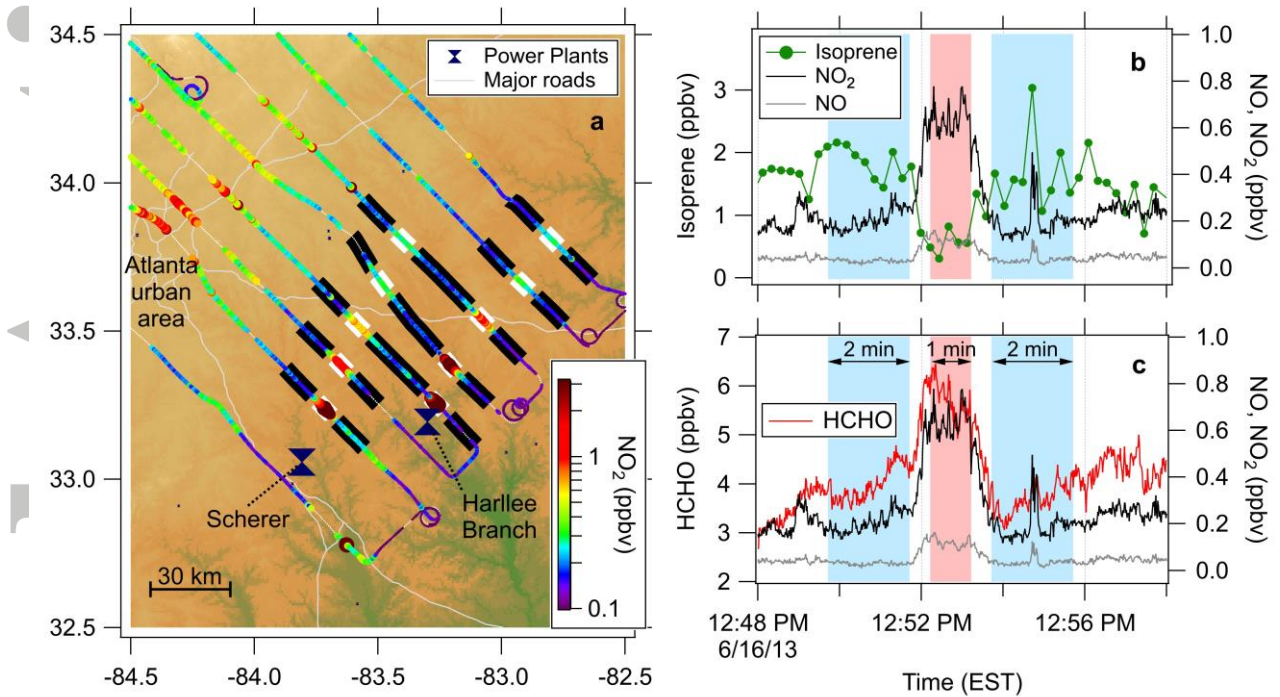
Warneke, C. et al. (2016), Instrumentation and measurement strategy for the NOAA SENEX aircraft campaign as part of the Southeast Atmosphere Study 2013, *Atmos. Meas. Tech.*, *9*, 3063–3093, doi:10.5194/amt-2015-388.

Whalley, L. K., Edwards, P. M., Furneaux, K. L., Goddard, A., Ingham, T., Evans, M. J., et al. (2011). Quantifying the magnitude of a missing hydroxyl radical source in a tropical rainforest. *Atmos. Chem. Phys.*, *11*, 7223–7233, <https://doi.org/10.5194/acp-11-7223-2011>.

Wolfe, G. M. et al. (2016), Formaldehyde production from isoprene oxidation across NO_x regimes, *Atmos. Chem. Phys.*, *16*, 2597–2610, doi:10.5194/acpd-15-31587-2015.

Xu, L., Middlebrook, A. M., Liao, J., de Gouw, J. A., Guo, H., Weber, R. J., et al. (2016). Enhanced formation of Isoprene-derived Organic Aerosol in Sulfur-rich Power Plant Plumes during Southeast Nexus (SENEX). *J. Geophys. Res.-Atmos.*, *121*, 11137–11153, <https://doi.org/10.1002/2016JD025156>.

Figure 1. Measurements downwind from the Scherer and Harlee Branch power plants on 16 June 2013. The wind direction on this day was from the southwest. (a) Flight track of the NOAA WP-3D aircraft color- and size-coded by the measured NO_2 onboard. The data used to calculate average mixing ratios of trace gases in- and outside the plumes are highlighted in white and black, respectively. Observations about 55 km downwind (third intercept) from the Scherer power plant showing (b) depletion in isoprene, and (c) enhancement in formaldehyde (HCHO) within the plume, which is accompanied by enhanced NO_2 and NO concentrations. The pink and blue coloring indicates the averaging times for data in- and outside the plume, respectively.



Accept

Figure 2. Evolution of NO₂, isoprene, formaldehyde (HCHO) and monoterpenes downwind from the Scherer and Harllee Branch power plants during the flight on 16 June 2013. Each of the data points corresponds to one of the plume intercepts shown in Figure 1a.

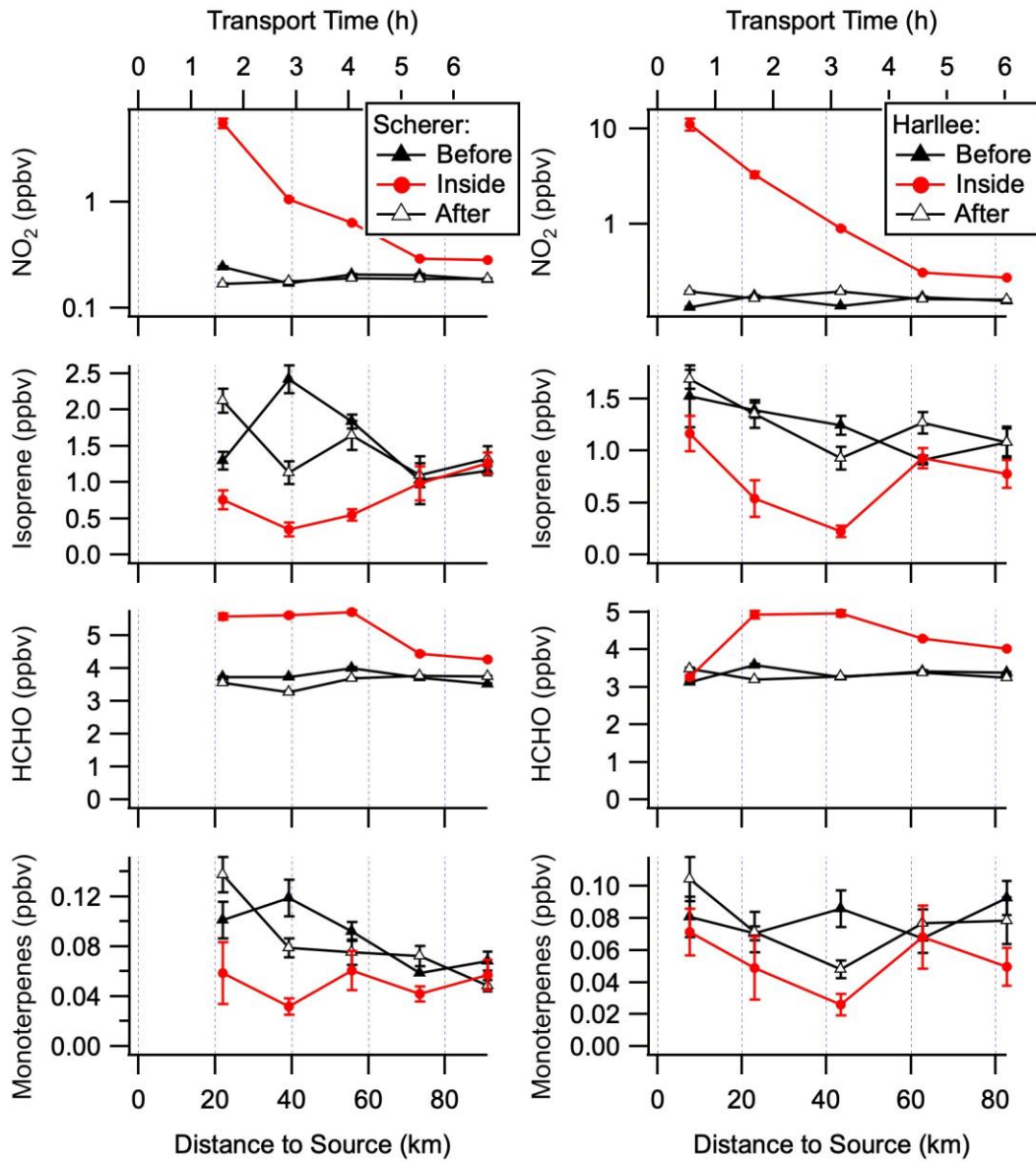


Figure 3. Hydroxyl enhancement ratio as a function of NO_2 mixing ratio determined from isoprene measurements (left) and monoterpene measurements (right) on 16 June 2013 downwind from the Harlee Branch and Scherer power plants as illustrated in Figure 1. The solid curves show fits of a lognormal distribution to the combined data from the two power plants with the asymptotic value set to one.

